http://doi.org/10.35784/iapgos.5302 received: 14.09.2023 | revised: 29.10.2023 | accepted: 30.11.2023 | available online: 20.12.2023

MODEL OF THE FLAT FAIRING ANTENNA DIELECTRIC LAYER WITH AERODYNAMIC HEATING

Valeriy Kozlovskiy[1], Valeriy Kozlovskiy[2], Oleksii Nimych[2], Lyudmila Klobukova[2], Nataliia Yakymchuk[3]
[1]National Technical University of Ukraine "Kyiv Polytechnic Institute named after Igor Sikorsky", Institute of Special Communications and Information Protection, Kyiv, Ukraine, [2]National Aviation University, Faculty of Cybersecurity, Computer and Software Engineering, Kyiv, Ukraine, [3]Lutsk National Technical University, Faculty of Computer and Information Technologies, Lutsk, Ukraine

Abstract. *To protect the antenna systems of modern aircraft, radio-transparent dielectric fairings are widely used. At low flight speeds, when designing and evaluating the characteristics of the fairing-antenna, it is assumed that the dielectric constant is a constant value and does not depend on the aircraft's flight speed. As the flight speed increases, as a result of aerodynamic heating of the fairing, its dielectric permeability changes, which leads to errors in the processing of received signals. Currently, to take into account the effect of dielectric coatings heating when designing antenna systems, the temperature of the fairing wall is averaged over its thickness. This method during maneuvering and at high flight speeds leads to large errors in determining the characteristics of the fairing antenna since the nature of the temperature distribution along the thickness of the fairing wall is not taken into account. A new approach to the analysis of dielectric layers with their uneven heating along the thickness is proposed. The obtained results make it possible to adjust the signal processing algorithms with analog and digital matrices, as a result of taking into account the emerging heat flows affecting the fairing of the aviation antenna, which leads to the improvement of the characteristics of the antenna systems.*

Keywords: aviation antenna, dielectric layer, aerodynamic heating, wave resistance, quadrupole

MODEL PŁASKIEJ WARSTWY DIELEKTRYCZNEJ ANTENY Z NAGRZEWANIEM AERODYNAMICZNYM

Streszczenie. *Aby chronić systemy antenowe nowoczesnych samolotów, szeroko stosuje się radioprzepuszczalne owiewki dielektryczne. Przy małych prędkościach lotu przy projektowaniu i ocenie charakterystyk anteny owiewkowej przyjmuje się, że stała dielektryczna jest wartością stałą i nie zależy od prędkości lotu samolotu. Wraz ze wzrostem prędkości lotu, w wyniku nagrzewania się aerodynamicznego owiewki, zmienia się jej przepuszczalność dielektryczna, co prowadzi do błędów w przetwarzaniu odbieranych sygnałów. Obecnie, aby uwzględnić wpływ nagrzewania powłok dielektrycznych przy projektowaniu systemów antenowych, temperaturę ścianki owiewki uśrednia się w stosunku do jej grubości. Metoda ta podczas manewrowania i przy dużych prędkościach lotu prowadzi do dużych błędów w określaniu charakterystyk anteny owiewki, gdyż nie bierze się pod uwagę charakteru rozkładu temperatury wzdłuż grubości ścianki owiewki. Zaproponowano nowe podejście do analizy warstw dielektrycznych przy ich nierównomiernym nagrzewaniu na całej grubości. Uzyskane wyniki pozwalają na dostosowanie algorytmów przetwarzania sygnału z matrycami analogowymi i cyfrowymi, w wyniku uwzględnienia powstających strumieni ciepła wpływających na owiewkę anteny lotniczej, co prowadzi do poprawy charakterystyki systemów antenowych.*

Słowa kluczowe: antena lotnicza, warstwa dielektryczna, nagrzewanie aerodynamiczne, opór falowy, kwadrupol

Introduction

At high flight speeds of aircraft (LA), aerodynamic heating of radio-transparent fairings (coatings) occurs. The reason for this is the influence of friction due to the viscosity of the air and the roughness of the fairing surface. The most intense heating of the material of the walls of the fairing leads to a change in the dielectric constant and losses, which is the reason for the change in the conditions for the passage of radio waves. As a result, the characteristics of the radome-antenna system differ from the calculated ones, which is an additional source of errors in the processing of received signals. The issue of taking into account this class of errors is especially acute in digital signal processing, when, during various types of aircraft maneuvers, the flight speed and altitude change, which leads to a change in the temperature of the fairing heating in time, as a result of which the characteristics of the fairing-antenna system also change in time. Thus, the problem of correcting the digital signal processing algorithm with an antenna array arises. For example, at different temperatures of heating the fairing wall above the elements of the antenna array, the delay time of the received signals changes, which leads to an increase in the direction finding errors of the phase direction finders. Obviously, with a change in the heating temperature, the value of the direction-finding error will also change.

The goal is to define a four-pole model of a flat dielectric layer during its aerodynamic heating. Representation of the layer in the form of a four-terminal network makes it possible to take into account the effect of temperature distribution on the passage of an electromagnetic field through a dielectric layer under various boundary conditions.

The paper poses the problem of finding the electro-magnetic field in a flat dielectric layer when a plane electromagnetic wave falls on its surface under conditions of aerodynamic heating. To solve the problem, it is first necessary to determine the distribution of temperature and permittivity over the thickness of the dielectric layer. Further, using the permittivity, we find the dependence of the wave resistance on the thickness and using the wave resistance, we determine the parameters of the equivalent quadrupole. The system of Z-parameters (resistance matrix) was chosen as the system of parameters of the quadrupole.

1. Literature review

In [1–25] are devoted to the issues of determining the electromagnetic field in the walls of the antenna radome and the creation of special radome materials, from which it follows that all materials used in the construction of microwave radomes can be divided into two groups [1, 5, 8, 10–12, 16, 20, 22, 23, 25, 26]: 1) structural materials that do not have an interaction device with an electromagnetic field during operation; 2) materials interacting with an electromagnetic field during aerodynamic heating, including with a laser. If there are no requirements for materials of the first group with their properties in the microwave, then for materials of the second group these requirements are mandatory, especially when it comes to millimeter microwaves and high-power pulsed lasers [2–4, 6, 7, 9, 13–15, 17–19, 21, 24, 25].

In the vast group of microwave materials, a special place is occupied by solid dielectrics, which are both structural materials that act as mechanical carriers of the structure and microwave materials operating in electromagnetic fields [2, 5, 7–9, 11–14, 17–20, 22–26].

Almost always, the most stringent requirements for the radio engineering parameters of dielectrics are imposed in connection with the special conditions of their operation. In particular, it should be noted the high requirements for the stability of the parameters and characteristics of dielectrics subjected to temperature effects. The properties of most of the known microwave dielectrics significantly depend on temperature, which ultimately changes the operational characteristics of radio engineering devices as a whole. This stimulates the development

of new heat-resistant and thermally stable dielectric materials [14, 17, 24] and the development of new methods and specialized research equipment for measuring at ultrahigh frequencies the temperature dependencies of material properties under thermophysical conditions similar to operational ones. Known methods for determining the temperature dependencies of the parameters of microwave dielectrics: waveguides, resonators, optical, and some others do not always solve the problem properly (there are unacceptably large measurement errors).

Existing methods [7, 8, 10–12, 16, 20, 24, 25] do not provide information about the dynamic dependence of the parameters of dielectric microwave materials on temperature during heating. It should be emphasized that the problem of measuring the parameters of dielectric materials when their physical state changes with simultaneous exposure to laser and microwave radiation have not been solved in modern microwave measuring technology. Research of this kind is often necessary for the theory and practice of designing various devices operating under conditions of aerodynamic heating.

At present, when designing fairings, aerodynamic heating is taken into account by averaging the temperature over the wall thickness [8, 22, 25], and the permittivity corresponding to the average temperature is used in calculations. The averaging method makes it possible to obtain satisfactory results under stationary flight conditions, when the heating temperature is constant throughout the thickness of the coating, that is, in the absence of a temperature gradient. When performing aircraft maneuvers, the conditions for heating the fairing change in time and wall thickness. In this case, the averaging method leads to large errors, since the change in the temperature gradient over time is not taken into account.

2. Researches methodology

When calculating electrodynamic objects, methods based on well-known solutions for a site of sufficiently small dimensions with a uniform distribution of the electric (E) and magnetic (H) fields are widely used. In this case, such an area can be replaced by a flat layer with a constant value of the vectors E and H. This layer, as an element of the fairing, is subjected to aerodynamic heating with an uneven temperature distribution over the thickness (figure 1), where T_1 is the temperature of the outer surface of the layer from the side of the heat flow, K; T_2 is the temperature of the inner surface of the layer, K. As the material of the layer, we choose quartz ceramics, which is widely used in the creation of fairings. It is known that the dependence of the absolute permittivity of quartz ceramics depends on temperature [10, 16, 20, 25].

$$\varepsilon(x) = \varepsilon_0 exp\left[1 - P + 2.6\cdot10^{-5}\left(T(x) - 290\right)\right] \tag{1}$$

where $T(x)$ is the temperature distribution, K; x – thickness of the dielectric layer; P – porosity (volume fraction of pores); ε_0 – absolute permittivity at zero porosity and T = 290 K. Numerical coefficient $2.6\cdot10^{-5}$ does not play a fundamental role and is determined by the type of material used.

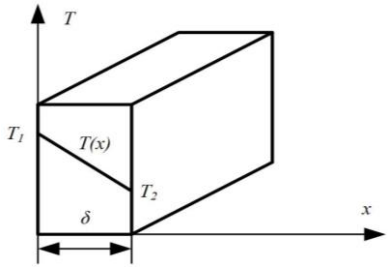

Fig. 1. Temperature distribution over the thickness of the dielectric layer

According to the law of temperature distribution over the layer thickness [6], we have

$$T(x) = (T_2 - T_1)\frac{x}{\delta} + T_1 \tag{2}$$

Substitute (2) into (1):

$$\begin{aligned}\varepsilon(x) = \varepsilon_0 \exp\left[1 - P + 2.6\cdot10^{-5}\left(T(x) - 290\right)\right] = \\ \varepsilon_0 \exp\left[1 - P + 2.6\cdot10^{-5}\left(T_1 - 290\right)\right]\cdot \\ \cdot\exp\left[2.6\cdot10^{-5}\left((T_2 - T_1)\frac{x}{\delta}\right)\right]\end{aligned} \tag{3}$$

Let us introduce the following notation:

$$A = 2.6\cdot10^{-5} \tag{4}$$

$$\begin{aligned}A_1 = 1 - P + 2.6\cdot10^{-5}\left(T_1 - 290\right) = \\ 1 - P + A\left(T_1 - 290\right)\end{aligned} \tag{5}$$

As a result, the permittivity can be written as:

$$\varepsilon(x) = \varepsilon_0 exp(A_1)\cdot exp\left[A\left((T_2 - T_1)\frac{x}{\delta}\right)\right] \tag{6}$$

Non-magnetic materials with an absolute magnetic permeability μ equal to the absolute magnetic permeability of a vacuum are usually used as dielectric coatings for aircraft antennas. In this case, the wave resistance of the layer at the normal incidence of a plane transverse wave, taking into account (6), is determined by the expression

$$\begin{aligned}W(x) = \sqrt{\frac{\mu}{\varepsilon(x)}} = \sqrt{\frac{\mu}{\varepsilon_0 exp(A_1)\cdot exp\left[A\left((T_2 - T_1)\frac{x}{\delta}\right)\right]}} = \\ = \sqrt{B}\exp\left[A\left((T_1 - T_2)\frac{x}{2\delta}\right)\right]\end{aligned} \tag{7}$$

Value

$$B = \frac{\mu}{\varepsilon_0 exp(A_1)} \tag{8}$$

Denote

$$2\alpha = A\left((T_1 - T_2)\frac{1}{2\delta}\right) = 2.6\cdot10^{-5}\left((T_1 - T_2)\frac{1}{2\delta}\right) \tag{9}$$

Then the wave resistance of the layer and the permittivity

$$W(x) = \sqrt{B}e^{2\alpha x},\ \varepsilon(x) = \varepsilon_0 e^{A_1}\cdot e^{-4\alpha x} \tag{10}$$

It follows from the analysis of expression (10) that the temperature difference on the outer and inner walls strongly affects the distribution of wave resistance over the layer thickness (figure 2).

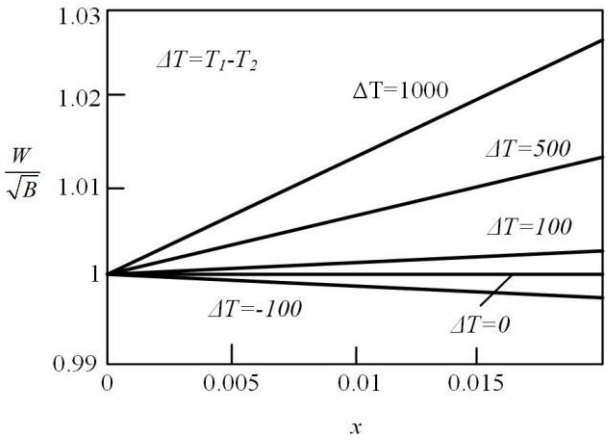

Fig. 2. Dependence of the wave resistance on the thickness of the dielectric layer with a total thickness of δ = 0.02 m

In the general case, processes in flat coatings under the incidence of an electromagnetic field that varies in time according to the harmonic law $e^{j\omega t}$, are described by the Maxwell equations:

$$rot\bar{H} = j\omega\varepsilon\bar{E},\ \ rot\bar{E} = j\omega\mu\bar{H} \tag{11}$$

where ε and μ are the absolute permittivity and permeability of the medium.

Let us assume that the parameters of the coverage environment change only along the z coordinate: $\varepsilon = \varepsilon(z), \mu = \mu(z)$. Consider the passage of a plane electro–magnetic wave (PEW) through an inhomogeneous layered medium. For definiteness, we assume that a plane wave has components E_x, H_y. Then equations (11) are transformed to the form

$$-\frac{dE_x}{dz} = j\omega\mu H_y,\quad -\frac{dH_y}{dz} = j\omega\varepsilon E_x \tag{12}$$

Let's introduce a new variable

$$\tau = \int_0^z \sqrt{\varepsilon(x)\mu(x)} \tag{13}$$

Obviously, τ is the propagation time of the plane wave from the beginning of the layer $(z = 0)$ to the points of the layer with the z coordinate, that is, the variable τ is the delay time of a layer of thickness z. In this case, the system of equations (12) takes the form:

$$-\frac{dE}{d\tau} = W(\tau)\, j\omega H,\quad -\frac{dH}{d\tau} = W^{-1}(\tau)\, j\omega E \tag{14}$$

where $W(\tau) = \sqrt{\mu(\tau)/\varepsilon(\tau)}$ is the wave impedance depending on the delay time τ, indices for E and H are omitted for simplicity.

Differentiating equations (14), we obtain equations for the strengths of the electric and magnetic fields E and H:

$$\mathrm{E}''(\tau) - \frac{\mathrm{W}'(\tau)}{\mathrm{W}(\tau)} E'(\tau) - p^2 E(\tau) = 0 \tag{15}$$

$$\mathrm{H}''(\tau) + \frac{\mathrm{W}'(\tau)}{\mathrm{W}(\tau)} H'(\tau) - p^2 H(\tau) = 0 \tag{16}$$

where $p = j\omega$ is a complex frequency variable.

Let's find the relationship between the delay time τ and layer thickness x. To do this, we substitute (6) with (13). In this case, since the heat flux propagates along the x-axis (figure 1), for convenience, we will assume that the layer is also inhomogeneous along the x-axis, that is, the PEW wave propagates along the x-axis. In this case, all formulas remain unchanged. The only components of the PEW field are E_y, H_z. Taking into account the above, we have the dependence of the delay time on the thickness (figure 3):

$$\begin{aligned}\tau &= \int_0^x \sqrt{\mu\varepsilon(\xi)}d\xi = \int_0^x \sqrt{\mu}\cdot\sqrt{\varepsilon_0\exp(\mathrm{A}_1)\cdot\exp(-4\alpha\xi)}d\xi = \\ &= \frac{b}{2\alpha}\left(1 - e^{-2\alpha x}\right),\ \ \mathrm{b} = \sqrt{\mu\varepsilon_0\exp(\mathrm{A}_1)}\end{aligned} \tag{17}$$

From formula (17) it follows that the delay time of the layer with thickness δ (figure 1) is equal to

$$\mathrm{t}_3 = \frac{b}{2\alpha}\left(1 - e^{-2\alpha\delta}\right) \tag{18}$$

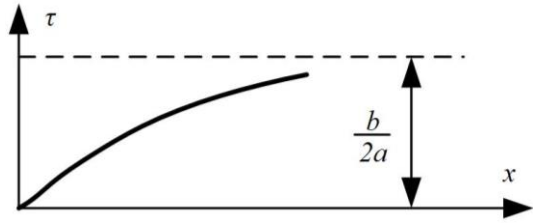

Fig. 3. Dependence of the delay time on the layer thickness

Using (17), we express the wave resistance $W(x)$ in terms of $W(\tau)$. For this, from expression (17) we find

$$-2\alpha x = \ln\left(1 - \tau\frac{2\alpha}{\mathrm{b}}\right) \tag{19}$$

Whence it follows that the wave resistance is determined by the expression

$$W(\tau) = \sqrt{B}e^{2\alpha x} = \sqrt{B}\frac{1}{1 - \dfrac{2\alpha}{b}\tau} \tag{20}$$

To determine the distribution of the electromagnetic field, we use equations (15), and (16). First, we find a solution for the electric field strength. To do this, we rewrite equation (15) in the form

$$\mathrm{E}''(\tau) - \frac{\mathrm{W}'(\tau)}{\mathrm{W}(\tau)} E'(\tau) + \omega^2 E(\tau) = 0 \tag{21}$$

According to (20), we find

$$\mathrm{W}'(\tau) = \frac{\mathrm{dW}(\tau)}{\mathrm{d}\tau} = \sqrt{B}\frac{\dfrac{2\alpha}{b}}{\left(1 - \dfrac{2\alpha}{b}\tau\right)^2} \tag{22}$$

where

$$\frac{\mathrm{W}'(\tau)}{\mathrm{W}(\tau)} = \frac{\dfrac{2\alpha}{b}}{1 - \dfrac{2\alpha}{b}\tau} = \frac{1}{\dfrac{b}{2\alpha} - \tau} \tag{23}$$

Substituting (23) into (21), we obtain the equation

$$\mathrm{E}''(\tau) + \frac{1}{\tau - \dfrac{\mathrm{b}}{2\alpha}} E'(\tau) + \omega^2 E(\tau) = 0 \tag{24}$$

Let us transform equation (24). To this end, we introduce a new variable

$$y = \tau - \frac{b}{2\alpha} \tag{25}$$

In this case

$$\frac{dE}{d\tau} = \frac{dE}{dy}\frac{dy}{d\tau} = \frac{dE}{dy},\quad \frac{d^2E}{d\tau^2} = \frac{d^2E}{dy^2}$$

and equation (21) takes the form

$$\mathrm{E}''(\mathrm{y}) + \frac{1}{y}E'(y) + \omega^2 E(y) = 0 \tag{26}$$

This equation is a modified Bessel equation, a particular solution of which is the zero-order Bessel function of the first kind $J_0(\omega y)$ [9]:

$$\frac{d^2 J_0(\omega y)}{dy^2} + \frac{1}{y}\frac{dJ_0(\omega y)}{dy} + \omega^2 J_0(\omega y) = 0 \tag{27}$$

The general solution to (26) is the function [9]

$$E(y) = C_1 J_0(\omega y) + C_2 Y_0(\omega y) \tag{28}$$

where $Y_0(\omega y)$ is the zero-order Bessel function of the second kind (the Neumann, Weber function). The constants C_1, C_2 are determined by the boundary conditions.

According to (14), the magnetic field strength is determined by the expression

$$H(\tau) = -\frac{E'(\tau)}{j\omega W(\tau)} \tag{29}$$

Returning to the variable τ, we rewrite (28)

$$\mathrm{E}(\tau) = C_1\omega J_0\left(\omega\left(\tau - \frac{\mathrm{b}}{2\alpha}\right)\right)C_2\omega Y_0\left(\omega\left(\tau - \frac{\mathrm{b}}{2\alpha}\right)\right) \tag{30}$$

To determine the magnetic field strength H, we use (29). Given that [25]

$$\begin{aligned}\frac{\mathrm{d}}{\mathrm{d}\tau}J_0\left(\omega\left(\tau - \frac{\mathrm{b}}{2\alpha}\right)\right) &= -\omega J_1\left(\omega\left(\tau - \frac{\mathrm{b}}{2\alpha}\right)\right) \\ \frac{\mathrm{d}}{\mathrm{d}\tau}\mathrm{Y}_0\left(\omega\left(\tau - \frac{\mathrm{b}}{2\alpha}\right)\right) &= -\omega Y_1\left(\omega\left(\tau - \frac{\mathrm{b}}{2\alpha}\right)\right)\end{aligned} \tag{31}$$

find

$$E'(\tau) = -C_1\omega J_1\left(\omega\left(\tau-\frac{b}{2\alpha}\right)\right) - C_2\omega Y_1\left(\omega\left(\tau-\frac{b}{2\alpha}\right)\right) \quad (32)$$

Therefore, according to (29)

$$H(\tau) = \left[C_1 J_1\left(\omega\left(\tau-\frac{b}{2\alpha}\right)\right) + C_2 Y_1\left(\omega\left(\tau-\frac{b}{2\alpha}\right)\right)\right]\cdot\frac{1-\frac{2a}{b}\tau}{j\sqrt{B}} \quad (33)$$

When analyzing a multilayer coating, it is convenient to represent it in the form of a cascade connection of four-terminal networks. In this case, each quadrupole is described by its system of parameters [18]: the system of Z-parameters, Y-parameters, the system of A-parameters (chain parameters), and various systems of wave parameters. At the same time, by knowing any system of parameters, it is possible to determine all the others. For definiteness, let's find the system of Z-parameters of one layer. Moreover, as Z-parameters, we take the surface resistance of the layer. In this case, according to (12...14), the layer can be represented as an inhomogeneous transmission line with a wave impedance $W(\tau)$ with voltage $U(\tau) = E(\tau)$ and current $I(\tau) = H(\tau)$. Let us agree that the potential of the upper terminal is greater than the potential of the lower terminal at the input and output of the quadrupole, and the input and output currents are directed towards the quadrupole. Then $E(\tau), H(\tau)$ there is a connection between [18]:

$$\begin{aligned} E(0) &= Z_{11}H(0) + Z_{12}H(t_з) \\ E(t_з) &= Z_{21}H(0) + Z_{22}H(t_з),\ Z_{12} = Z_{21} \end{aligned} \quad (34)$$

In general, the surface resistance of the layer, as follows from (30, 33), is equal to

$$Z_{in}(\tau) = \frac{C_1 J_0\left(\omega\left(\tau-\frac{b}{2\alpha}\right)\right) + C_2 Y_0\left(\omega\left(\tau-\frac{b}{2\alpha}\right)\right)}{\left[C_1 J_1\left(\omega\left(\tau-\frac{b}{2\alpha}\right)\right) + C_2 Y_1\left(\omega\left(\tau-\frac{b}{2\alpha}\right)\right)\right]\frac{1-\frac{2a}{b}\tau}{j\sqrt{B}}} \quad (35)$$

where the constants C_1, C_2 are determined by the surface resistance of the adjacent medium Z_a (the medium at the point $\tau = t_з$). Assuming $\tau = t_з$ we have

$$Z_a = \frac{C_1 J_0\left(\omega\left(t_з-\frac{b}{2\alpha}\right)\right) + C_2 Y_0\left(\omega\left(t_з-\frac{b}{2\alpha}\right)\right)}{\left[C_1 J_1\left(\omega\left(t_з-\frac{b}{2\alpha}\right)\right) + C_2 Y_1\left(\omega\left(t_з-\frac{b}{2\alpha}\right)\right)\right]\frac{1-\frac{2a}{b}t_з}{j\sqrt{B}}} \quad (36)$$

Let us express the input resistance $Z_{in}(\tau)$ in terms of the surface resistance of the adjacent medium Z_a, C_1, C_2. Then, according to (30, 33), we can write

$$\begin{aligned} &C_1 J_0\left(\omega\left(t_з-\frac{b}{2\alpha}\right)\right) + C_2 Y_0\left(\omega\left(t_з-\frac{b}{2\alpha}\right)\right) = E(t_з) \\ &\left[C_1 J_1\left(\omega\left(t_з-\frac{b}{2\alpha}\right)\right) + C_2 Y_1\left(\omega\left(t_з-\frac{b}{2\alpha}\right)\right)\right]\frac{1-\frac{2a}{b}t_з}{j\sqrt{B}} = H(t_з) \end{aligned} \quad (37)$$

From the system of equations (37) and expression (36), we find

$$C_1 = H_a\frac{Z_a Y_1 - \frac{Y_0}{F(t_з)}}{J_0Y_1 - J_1Y_0},\quad C_2 = H_a\frac{\frac{J_0}{F(t_з)} - Z_a J_1}{J_0Y_1 - J_1Y_0} \quad (38)$$

where the function argument J_0, J_1, Y_0, Y_1 is $\omega\left(t_з-\frac{b}{2\alpha}\right)$ (37).

Value $F(\tau)$ is defined by the expression

$$F(\tau) = \frac{1-\frac{2a}{b}\tau}{j\sqrt{B}} \quad (39)$$

Thus, the surface resistance (35) is transformed into the form

$$Z_{in}(\tau) = \frac{\left(Z_a Y_1 - \frac{Y_0}{F(t_з)}\right)J_0\left(\omega\left(\tau-\frac{b}{2\alpha}\right)\right) + \left(\frac{J_0}{F(t_з)} - Z_a J_1\right)Y_0\left(\omega\left(\tau-\frac{b}{2\alpha}\right)\right)}{\left[\left(Z_a Y_1 - \frac{Y_0}{F(t_з)}\right)J_1\left(\omega\left(\tau-\frac{b}{2\alpha}\right)\right) + \left(\frac{J_0}{F(t_з)} - Z_a J_1\right)Y_1\left(\omega\left(\tau-\frac{b}{2\alpha}\right)\right)\right]F(\tau)} \quad (40)$$

Using (40) we find the elements of the Z-parameter system (34). An element Z_{11} at an arbitrary value of the coordinate τ is determined by expression (40) at $Z_a = \infty$.

$$Z_{11}(\tau) = \frac{Y_1\left(\omega\left(t_з-\frac{b}{2\alpha}\right)\right)J_0\left(\omega\left(\tau-\frac{b}{2\alpha}\right)\right) - J_1\left(\omega\left(t_з-\frac{b}{2\alpha}\right)\right)Y_0\left(\omega\left(\tau-\frac{b}{2\alpha}\right)\right)}{\left[Y_1\left(\omega\left(t_з-\frac{b}{2\alpha}\right)\right)J_1\left(\omega\left(\tau-\frac{b}{2\alpha}\right)\right) - J_1\left(\omega\left(t_з-\frac{b}{2\alpha}\right)\right)Y_1\left(\omega\left(\tau-\frac{b}{2\alpha}\right)\right)\right]F(\tau)} \quad (41)$$

To define elements Z_{22}, Z_{12} we use (40). To do this, we find the layer resistance under the condition that $Z_a = 0$, $Z_a = R$, where R is a positive real number (resistance).

Then the short circuit layer resistance $Z_{sc}(Z_a = 0)$ $Z_R(Z_a = R)$ can be expressed in terms of the elements of the resistance matrix [18]:

$$Z_{sc} = Z_{11} - \frac{Z_{12}^2}{Z_{22}},\ Z_R = Z_{11} - \frac{Z_{12}^2}{Z_{22}+R} \quad (42)$$

From the system (42) we find the elements Z_{22}, Z_{12}:

$$Z_{22} = \frac{R(Z_{11}-Z_R)}{Z_R - Z_{sc}},\ Z_{12}^2 = \frac{R(Z_{11}-Z_R)(Z_{11}-Z_{sc})}{Z_R - Z_{sc}} \quad (43)$$

$$Z_{sc}(\tau) = \frac{-Y_0\left(\omega\left(t_з-\frac{b}{2\alpha}\right)\right)J_0\left(\omega\left(\tau-\frac{b}{2\alpha}\right)\right) + J_0\left(\omega\left(t_з-\frac{b}{2\alpha}\right)\right)Y_0\left(\omega\left(\tau-\frac{b}{2\alpha}\right)\right)}{\left[-Y_0\left(\omega\left(t_з-\frac{b}{2\alpha}\right)\right)J_1\left(\omega\left(\tau-\frac{b}{2\alpha}\right)\right) + J_0\left(\omega\left(t_з-\frac{b}{2\alpha}\right)\right)Y_1\left(\omega\left(\tau-\frac{b}{2\alpha}\right)\right)\right]F(\tau)} \quad (44)$$

Thus, expressions (41)–(44) completely determine the elements of the resistance matrix of a four-terminal network formed by a dielectric layer during aerodynamic heating.

3. Experiments

Based on the results obtained, the influence of aerodynamic heating of the radome of a two-element antenna array (AR), figure 4, on determining the angle of wave arrival was studied.

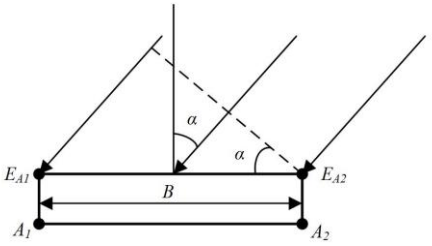

Fig. 4. Two-element antenna array under the dielectric layer

The absolute error in determining the direction of arrival of the wave that occurs when the aerodynamic heating of the fairing is not taken into account is determined by the expression

$$\Delta\phi = \phi_0 - \alpha = \arcsin\frac{(\Delta\Phi + \beta_1 - \beta_2)\lambda}{2\pi B} - \arcsin\frac{\Delta\Phi\lambda}{2\pi B},\ \Delta\Phi = \frac{2\pi B}{\lambda}\sin\alpha \quad (45)$$

where β_1, β_2 are the arguments of the dielectric transmission coefficient over the element A_1, A_2, respectively; ϕ_0 – the angle of arrival of the wave, calculated taking into account the heating of the fairing, α – the angle of arrival of the wave, calculated without taking into account the heating of the fairing.

P9606 pyroceramic (USA) with a relative permittivity at porosity $P = 0\%$ equal to $\varepsilon_r = 5.8$, oscillation frequency $f = 10$ GHz was used as the fairing material.

4. Results

On figures 5–8 show the dependences of the angular error of arrival of the TE wave on various factors.

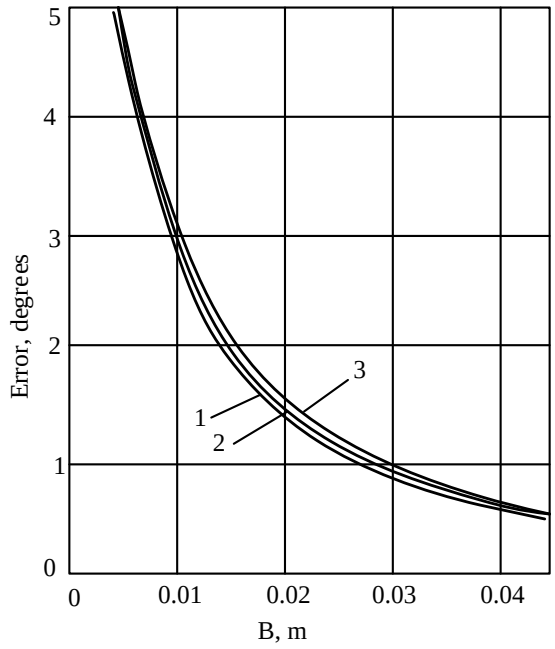

Fig. 5. Dependence of the angular error on the base (meter) at different angles of wave incidence: 1 – $\varphi_0 = \pi/16$, 2 – $\varphi_0 = \pi/8$; 3 – $\varphi_0 = \pi/3$; oscillation frequency $f = 10$ GHz; the heating temperature of the dielectric above the lattice element A_1 is $T_1 = 290$ K, and above the element A_2 – $T_2 = 1000$ K

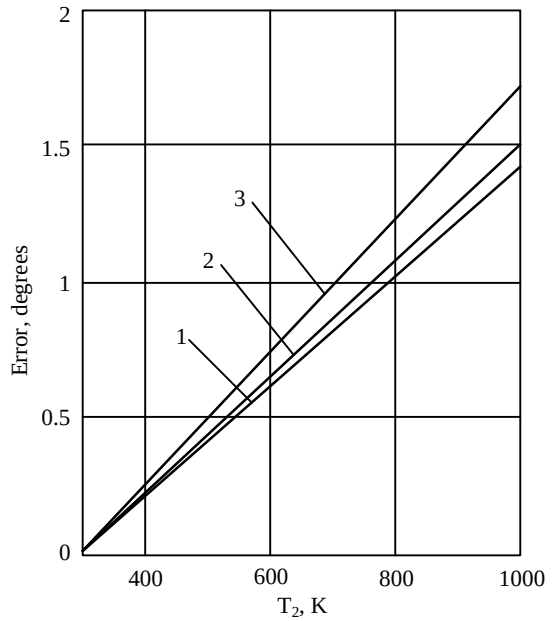

Fig. 6. Dependence of the angular error on temperature T_2 at $T_1 = 290$ K, $B = 0.015$ m, $P = 30\%$, material – P9606 pyroceramic, oscillation frequency $f = 10$ GHz: $\varphi_0 = \pi/16$; 2 – $\varphi_0 = \pi/4$; 3 – $\varphi_0 = \pi/3$

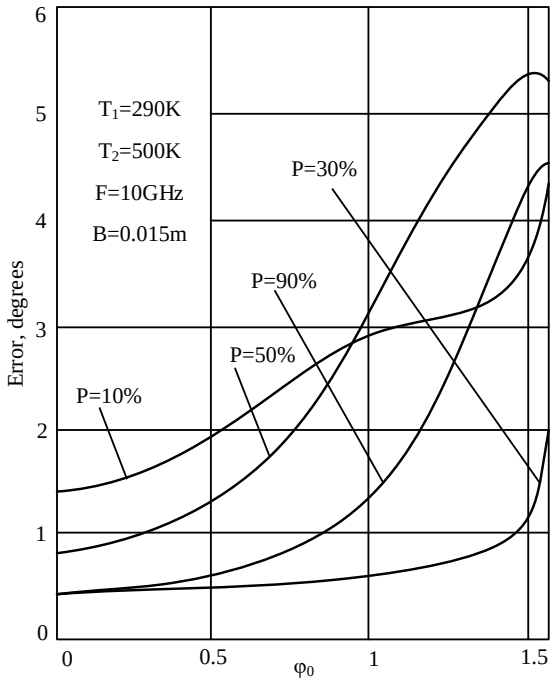

Fig. 7. Dependence of the angular error on the angle of incidence of the wave at different porosities P, material – P9606 pyroceramic

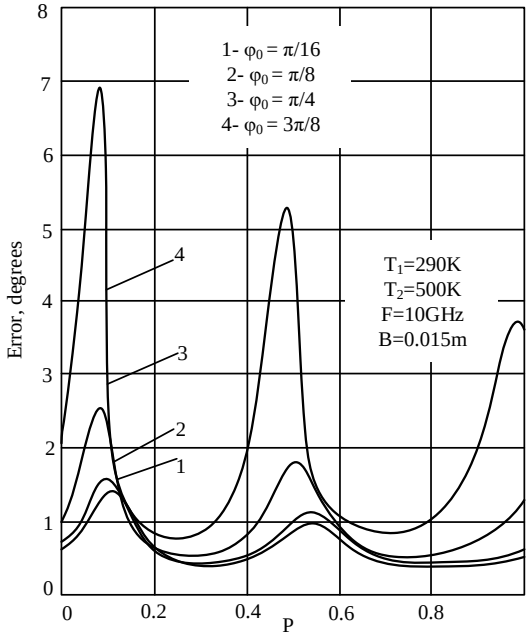

Fig. 8. Dependence of the angular error on porosity for P9606 pyroceramics at various angles of incidence φ_0

5. Discussion

It follows from the dependences in figures 5–8 that the angular error in determining the arrival of an electromagnetic wave depends not only on the size of the AA base, but also on the temperature of the aerodynamic heating of the dielectric wall of the fairing, the porosity of the dielectric, and the angle of arrival of the wave. From the analysis of the obtained dependencies, it follows:

1. With an increase in the temperature difference between heating the dielectric over various elements of the AR, the angular error increases according to a lawyer close to linear. In this case, with an increase in the angle of arrival of the wave, the angular error also increases.

2. With an increase in the angle of incidence of the wave at a constant porosity, the angular error also increases. In this case, the minimum error is observed at normal wave incidence (the angle of incidence is zero $\phi_0 = 0$), and the maximum is observed near the angles of incidence $\phi_0 = \pi/2$. There are ranges of wave incidence angles at which different porosities correspond to the same angular errors. For example, at $P = 10\%$, 50%, and the angle of incidence $\phi_0 = 0.8$ is rad, the angular error is 2.8 degrees. Moreover, at $\phi_0 < 0.8$ rad, the angular error at porosity $P = 10\%$ exceeds the angular error at $P = 50\%$, and $\phi_0 > 0.8$ vice versa at rad.

3. When the porosity changes from 0 to 100%, the angular error has three maxima and two minima at different wave incidence angles. The error maxima are concentrated in the porosity ranges (5%–15%), (45%–55%), and (95%–100%). In other areas of porosity values, we have minimal angular errors (figure 8).

4. The current state of the theory of aerodynamic heating of a dielectric [5, 8, 10, 14, 19, 20, 22, 23, and 25] does not allow establishing clear analytical relationships between the electrical characteristics of a dielectric and such external influencing factors as temperature, pressure, substance density, frequency of an external electromagnetic field. There are no prerequisites that make it possible to analytically formalize the temperature dependences of ε and $tg\delta$ of dielectrics with a partial change in the phase and state of the material as a result of high-temperature heating. On the way to solving this complex problem, there are significant theoretical difficulties that have not yet been overcome. The available information on the temperature dependences of ε and $tg\delta$ corresponds only to slow temperature changes and does not in any way reflect the properties of the material during thermal heating (pulsed mode of turning the laser beam on and off) or thermal shock.

Operating experience and numerous theoretical and experimental studies [1–4, 7, 8, 11, 13, 15, 16, 21, 24–26] have shown that when heated, fairings made of even the best dielectric materials noticeably change the radiation characteristics of the antennas they protect. In this case, the temperature dependences $\varepsilon(T)$ and $tan\delta(T)$ are determined experimentally for different thicknesses x of the dielectric layer. The obtained results are averaged over the thickness of the fairing wall. This method is time-consuming and inaccurate due to the low reliability of the dielectric parameters calculation and the disregard for heat distribution processes.

The approach developed in this work is based on the use of the law of thermal conductivity [6] with the distribution of temperature over the thickness of the dielectric layer (2) and the use of the known temperature dependence of the permittivity (1). The numerical coefficient in (1) is determined by the type of dielectric. In the general case, by choosing the coefficients A, A_1 in formula (6), one can write an expression for the permittivity of various ceramic materials.

The obtained relations, in contrast to the known solutions [5, 8, 20, 22, 23, 25] make it possible to represent the dielectric layer during aerodynamic heating in the form of a four-terminal network with elements of the resistance matrix (41)–(44), which makes it possible to increase the accuracy of calculations of antenna-radome systems for by taking into account the process of heat distribution over the thickness of the dielectric wall.

6. Conclusions

Development task solved models of a flat dielectric layer of a fairing under aerodynamic heating.

The scientific novelty lies in the fact that for the first time, a model of a flat dielectric layer in the form of a four-terminal network has been developed, which takes into account the gradient distribution of heat over the layer thickness. In this case, the four-terminal network is an inhomogeneous transmission line with an exponential change in the wave resistance along the thickness and depends on the temperature difference at the boundaries of the dielectric layer.

The practical value of the obtained results consists in increasing the accuracy of calculations of the radome during aerodynamic heating, which makes it possible to design antenna-radome systems for moving objects with the required radiation pattern under conditions of uneven heating of the radome wall. The research results can be used in the development of space communication and navigation systems with increased accuracy characteristics compared to existing analogs.

Prospects for further research are related to the development of analog and digital radome-antenna systems with increased angular accuracy, operating under conditions of aerodynamic heating.

References

[1] Akan V., Yazgan E.: Antennas for Space Applications: A Review. Advanced Radio Frequency Antennas for Modern Communication and Medical Systems, IntechOpen, 2020, [http://doi.org/10.5772/intechopen.93116].
[2] Chahat N.: A mighty antenna from a tiny CubeSat grows. IEEE Spectrum 55, 2018, 33–37 [http://doi.org/10.1109/MSPEC.2018.8278134].
[3] Deng J., Zhou G., Qiao Y.: Multidisciplinary design optimization of sandwich-structured radomes. Institution of Mechanical Engineers, Part C: Journal of Mechanical Engineering Science 233(1), 2019, 179–189 [http://doi.org/10.1177/0954406218757268].
[4] Dippong T. et al.: Thermal behavior of Ni, Co and Fe succinates embedded in silica matrix. J. Therm. Analysis. Calorim. 136, 2019, 1587–1596 [http://doi.org/10.1007/s10973-019-08117-8].
[5] Escalera A. S. et al.: Effects of Radome Design on Antenna Performance in Transonic Flight Conditions. AIAA 2020-2187. AIAA Scitech 2020 Forum, 2020 [http://doi.org/10.2514/6.2020-2187].
[6] Gilchuk A. V., Khalatov A. A.: Theory of thermal conductivity. NTUU KPI named after Igor Sikorsky, 2017.
[7] Grinevich A. V., Lavrov A. V.: Evaluation of the ballistic characteristics of ceramic materials. Proceedings of VIAM 3(63), 2018, 95–102 [http://doi.org/10.18577/2307-6046-2018-0-3-95-102].
[8] Gyulmagomedov N. K.: Influence of the radiotransparent radome on characteristics of radar station. AIP Conference Proceedings 2318, 2021, 180001 [http://doi.org/10.1063/5.0036566].
[9] Korn G.: Handbook of mathematics for scientists and engineers: Definitions, theorems, formulas. Book on Demand, 2014.
[10] Li H. Y. et al.: Ameliorated Mechanical and Dielectric Properties of Heat-Resistant Radome Cyanate Composites. Molecules 25, 2020, 3117.
[11] Li H. Y. et al: Ameliorated Mechanical and Dielectric Properties of Heat-Resistant Radome Cyanate Composites. Molecules 25(14), 2020, 3117 [http://doi.org/10.3390/molecules25143117].
[12] Lu Y. et al.: A Study on the Electromagnetic–Thermal Coupling Effect of CrossSlot Frequency Selective Surface. Materials 15, 2022, 640 [http://doi.org/10.3390/ma15020640].
[13] Meyer G. J.: Polyurethane Foam: Dielectric Materials for Use in Radomes and Other Applications. General Plastics Manufacturing Company, 2015.
[14] Nair R. U. et al.: Temperature-dependent electromagnetic performance predictions of a hypersonic streamlined radome. Prog. electromagn. Res. 154, 2015, 65–78.
[15] Narendara S., Gopikrishna R.: Evaluation of structural integrity of tactical missile ceramic radomes under combined thermal and structural loads. Procedia Structural Integrity 14, 2019, 89–95.
[16] NASA Outgassing Data for Selecting Spacecraft Materials, https://outgassing.nasa.gov (available: April 20, 2020).

[17] Öziş E. et al.: Metamaterials for Microwave Radomes and the Concept of a Metaradome: Review of the Literature. International Journal of Antennas and Propagation 2017, ID1356108 [http://doi.org/10.1155/2017/1356108].
[18] Plonus M.: Electronics and Communications for Scientists and Engineers, 2020 [http://doi.org/10.1016/C2018-0-00442-9].
[19] Raveendranath U. N. et al.: Temperature-Dependent Electromagnetic Performance Predictions of a Hypersonic Streamlined Radome. Progress In Electromagnetics Research 154, 2015, 65–78.
[20] Romashin A. G. et al.: Radiotransparent fairings for aircraft. National Aerospace University, Kharkov 2003.
[21] Seckin S. et al.: Dielectric Properties of Low-Loss Polymers for mmW and THz Applications. International Journal of Infrared and Millimeter Waves 40, 2019, 557–573 [http://doi.org/10.1007/s10762-019-00584-2].
[22] Tahseen H. U. et al.: Design of FSS-antenna-radome system for airborne and ground applications. LET Communications, 2021 [http://doi.org/10.1049/cmu2.12181].
[23] Tahseen H. U. et al.: Design of FSS-antenna-radome system for airborne and ground applications. IET Commun. 2021, 15, 1691–1699, [http://doi.org/10.1049/cmu2.12181].
[24] Xu W. et al.: Study on the electromagnetic performance of inhomogeneous radomes for airborne applications part 1: Characteristics of phase distortion and boresight error. IEEE Transactions on Antennas and Propagation 65(6), 2017, 3162–3174.
[25] Ya M. et al.: Physics of heating microwave dielectrics of aircraft and their protection. SSGA, Novosibirsk 2008.
[26] Zhang H. X. et al.: Massively Parallel Electromagnetic–Thermal Cosimulation of Large Antenna Arrays. IEEE Antennas Wire. Propag. Lett. 19, 2020, 1551–1555.

D.Sc. Valerii Kozlovskiy
e-mail: valerey@ukr.net

Research interests: radio electronics, ultra-high frequencies techniques, nonregular distributed circles.

http://orcid.org/0000-0003-0234-415X

D.Sc. Valeriy Kozlovskiy
e-mail: vvkzeos@gmail.com

Research interests: telecommunication systems, programmable logic controllers, research network security, features of the communication lines organization and operation.

http://orcid.org/0000-0002-8301-5501

Oleksii Nimych
e-mail: aleksei.nimich@gmail.com

Research interests: cybersecurity, software engineering, antenna systems

http://orcid.org/0000-0003-1759-7088

Liudmyla Klobukova
e-mail: klp@nau.edu.ua

Research interests: telecommunications and information technologies, multichannel communication systems, orthogonal modulation

http://orcid.org/0000-0001-9799-4387

Ph.D. Natalia Yakymchuk
e-mail: n.yakymchuk@lntu.edu.ua

Research interests: diagnostics and control of the telecommunication networks state, end-to-end diagnostics, congestion management.

http://orcid.org/0000-0002-8173-449X